PROCEEDINGS, Eighteenth Workshop on Geothermal Reservoir Engineering
Stanford University, Stanford, California, January 26-28, 1993
SGP-TR-145

CORE IMAGE ANALYSIS OF MATRIX POROSITY IN THE GEYSERS RESERVOIR

Dennis L. Nielson, Greg Nash, Jeffrey B. Hulen and Alan C. Tripp

University of Utah Research Institute
391-C Chipeta Way
Salt Lake City, Utah 84108

ABSTRACT

Adsorption is potentially an important consideration when calculating reserves at The Geysers. Our investigations of the mineralogical relationships in core samples have shown matrix pore spaces to be largely associated with fractures. Dissolution of calcite from hydrothermal veins increases porosity in the graywacke reservoir. The high relative surface area of secondary alteration phases could promote adsorption. In order to quantify porosity distribution and surface area, Scanning Electron Microscope (SEM) images were analyzed using software developed for the interpretation of satellite imagery. This software classifies the images as either crystal or pore and then accumulates data on pore size, total porosity and surface area of the mineral-pore interface. Review of literature shows that data on thickness of adsorbed water layer does not exist for many of the mineral phases of interest in The Geysers. We have assumed thicknesses of 10, 100, and 5300 Angstroms for the adsorbed layer and calculated the relative proportions of adsorbed water. These calculations show 0.005%, 0.05%, and 2.5% of total water would be adsorbed using the above thicknesses.

INTRODUCTION

The Geysers vapor-dominated geothermal system is conceptualized in terms of a dual-porosity model where steam is present in major through-going fractures, is highly mobile under production conditions and is the pressure-controlling phase. Liquid water, by contrast, occupies pores in the matrix between these fractures and is largely an immobile phase (Truesdell and White, 1973; Pruess and Narasimhan, 1982). Buffering of the steam at saturated pressure and temperature conditions prior to exploitation demonstrated that the steam is flashing from a liquid reservoir in response to production. The majority of the heat reserves in the reservoir are in the rock and transfer to the steam through the process of flashing. Total reservoir production therefore will be determined by the water content of the reservoir, which is a function of matrix porosity. Although fractures are responsible for extremely rapid and widespread communication within the reservoir, they have not effectively breached either the cap or lateral permeability seals, and the reservoir is generally acknowledged to have little natural recharge (Williamson, 1990).

Recent pressure declines at The Geysers have raised the question of the longevity of the steam field and the most effective means of injection into the resource to prolong its economic life. The potential importance of liquid-water adsorption in reservoir storage has been discussed by a number of researchers (Economides and Miller, 1985; Ramey, 1990) who argue that failure to consider adsorption will lead to underestimation of reserves. Pruess and O'Sullivan (1992) have surveyed the literature on capillarity and adsorption on rock surfaces and point out that there is a large variation in the degree of adsorption in rocks that they attribute to different pore size distribution and variations in composition and activity of mineral surfaces. They also feel that vapor pressure lowering will only become a significant process at liquid saturations of 20% or less and is thus only important during the final stages of reservoir production.

The porosity of reservoir rocks at The Geysers has been determined by standard core analyses (Gunderson, 1990). Gunderson reports an average porosity of 2.3% (range of 0.6% to 5.8%) in the graywacke reservoir. The felsite reservoir has an average porosity of 2% (range of 1.7% to 4.2%). Porosity in the graywacke was found to decrease with increasing depth and with proximity to the felsite. Gunderson also presented a schematic representation of four types of matrix porosity from The Geysers core. A revision of this diagram based on the results of Hulen et al. (1991,1992) and this study is shown in Figure 1. Matrix porosity in the reservoir is largely a function of three different processes. Creation of new void space through rock brecciation (tectonic or hydrothermal) as well as dissolution of calcite, enhances porosity. Precipitation of silicate phases within the pores decreases porosity, but may enhance adsorption.

Core samples from the reservoir show that matrix porosity is heterogeneous. Dissolution of Franciscan calcite produces pores that are more or less randomly distributed through the graywacke. Calcite dissolution from veins forms the largest pores within the vein, but also forms pores marginal to the veins. Unmineralized fractures are porous within and along the fracture. Closely spaced fractures, in addition, are often separated by areas of high matrix porosity. We do not have access to core that samples a steam entry within the normal graywacke reservoir. Since the highest matrix porosity is associated with fracturing, the results of our work probably underestimate total porosity.

Our observations of The Geysers cores also suggest that there is a stratigraphic distribution for matrix porosity. Figure 2 is a schematic diagram showing our concept of porosity within the reservoir. As illustrated in Figure 1, porosity in the graywacke reservoir results from the dissolution of previously existing calcite as well as tectonic and hydrothermal fracturing. An important

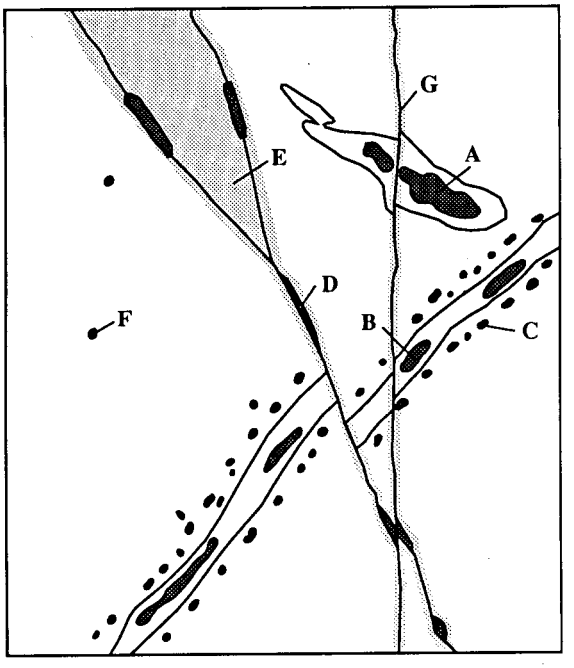

Figure 1 - Schematic diagram of "matrix" porosity in The Geysers normal graywacke reservoir. **A** is pore space created by dissolution of Franciscan calcite in discontinuous pods. **B** is pore space formed form dissolution of calcite in quartz + calcite veins. **C** are pores marginal to the quartz + calcite veins. **D** is porosity in small, partially sealed fractures, and **E** represents the porosity between and adjacent to these young fractures. **F** represents isolated pores. **G** are unmineralized fractures that are the youngest in the field. Modified from Gunderson (1990).

aspect of this portion of the reservoir is the development of low-angle fractures discussed by a number of authors (see Nielson and Brown, 1990 for a summary). Alternatively, we suggest that flat fractures may be developed by strike-slip faulting and generation of associated "flower" structures (Willis and Tosdal, 1992). In the hornfels zone, prograde reactions resulted in conversion of calcite to calc-silicate minerals during contact metamorphism and metasomatism associated with emplacement of the felsite. Matrix porosity here, then, is largely confined to brecciated areas associated with faulting that followed the emplacement of the felsite. Matrix porosity in the felsite, reported by Gunderson (1990), is probably associated with faults and joints or miarolitic cavities. Thus, matrix porosity and associated liquid reserves, are probably highest in the graywacke.

Hulen et al. (1991,1992) have described very intricate and delicate mineral textures within vugs that constitute the matrix porosity of the reservoir rocks. Since adsorption is a function of surface-energy relationships among solid, liquid and vapor phases, it seems likely that mineral species and textures will influence the storage capacity of the reservoir.

OBSERVATIONS

The textural relationships for several mineral phases are shown in Scanning Electron Microscope (SEM) images

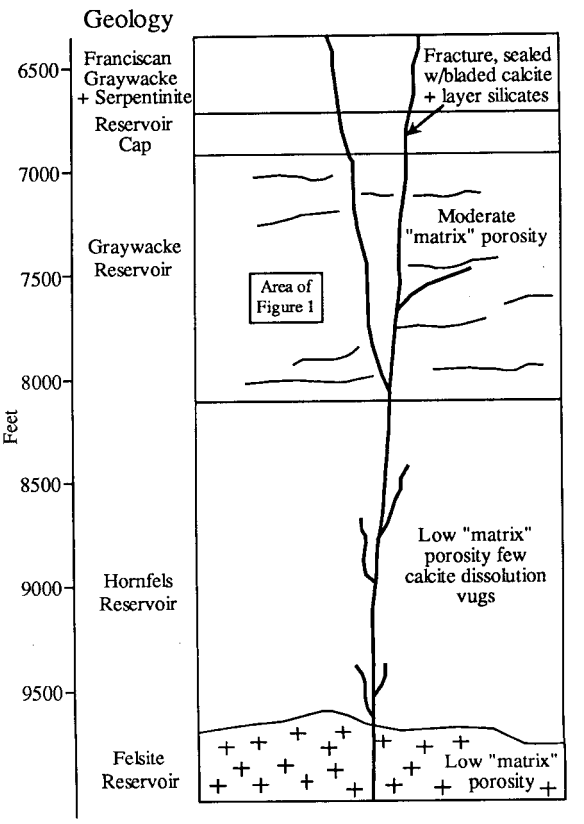

Figure 2 - Reservoir model of The Geysers

in Figure 3. The most common hydrothermal phases in the reservoir are actinolite, epidote, and quartz. Bladed calcite, wairakite and layer silicates are more common in the cap at the top of the reservoir (Hulen et al., 1991). Figure 3a shows the texture formed by actinolite growing within a solution vug while Figure 3b shows the texture formed by epidote in a similar setting. Figures 3c and d show two magnifications of pore space in a sample where the surface has been polished to emphasize the location and geometry of the overall porosity. The pore space is confined to a hydrothermal vein. SEM and thin-section examination of the rock matrix shows that porosity is generally not present along the margins of the original sedimentary grains. This is an important distinction between The Geysers reservoir and conventional siliciclastic hydrocarbon reservoirs.

The observation of these textures suggests that porosity measurements on core only partially describe the relationships necessary to understand reservoir storage. The pore size, size distribution and surface areas of minerals should influence adsorption and capillarity. We have based our measurements of pore characteristics on the interpretation methods described in Krohn and Thompson (1986), Krohn (1988) and Thompson (1991). These works demonstrated a fractal distribution for porosity in a suite of sandstones. However, we have improved upon their image analysis techniques to enable calculations of surface area as well as pore volume.

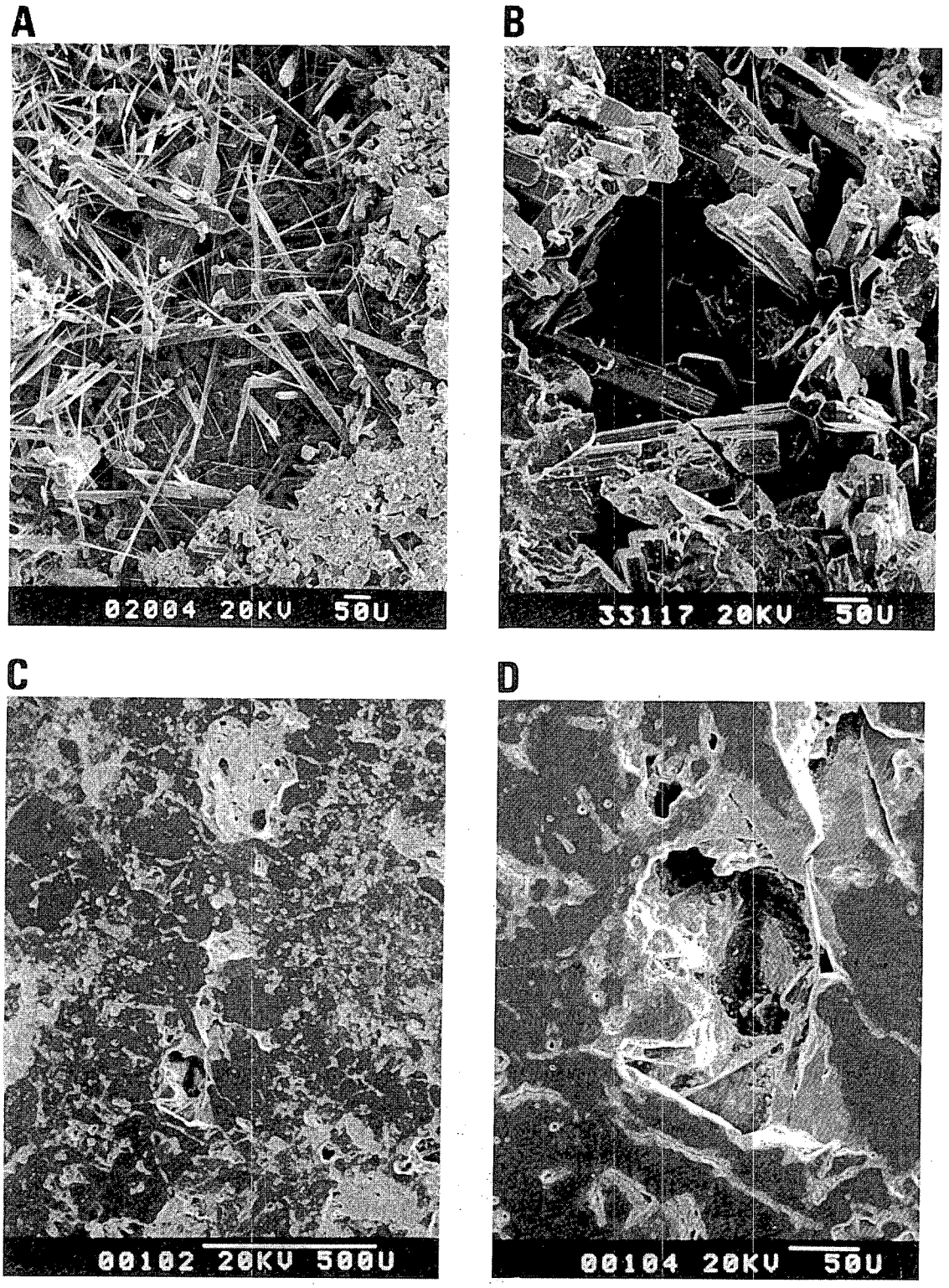

Figure 3. SEM images of core from The Geysers reservoir
A. Actinolite in dissolution pore from well Prati-State 12
B. Epidote in dissolution pore from well NEGU-17
C. Polished sample of vein with dissoution pores from well NEGU-17
D. Same sample as C, higher magnification

ADSORPTION

Adsorption on surfaces can be considered to result from the physical attraction between a liquid or a gas and the solid substrate. The process results in three thermodynamically distinct phases: the solid, adsorbed liquid (or gas) and liquid (or gas) (Jaroniec and Madey, 1988). The theoretical details of the adsorption process can get very complex for The Geysers system, and a comprehensive discussion is beyond the scope of this paper. Different crystallographic orientations of the same mineral will have different adsorption capacities, as will different mineral phases. The adsorbed fluid in The Geysers reservoir is also likely to be chemically variable as evidenced by the chemical differences of fluids trapped within fluid inclusions (Moore, 1992). Thus, complex relationships of electrolyte adsorption would have to be considered in a comprehensive treatment of the reservoir.

The thickness of the adsorbed layer is of considerable interest in determining the potential adsorbed fluid reserves. There are few data that are of use in determining this for the minerals and fluid compositions present in The Geysers field. A conservative approach is to consider adsorption of one molecular layer. He et al. (1987) concluded from a study of tuff that beyond 7 to 8 Angstroms from the mineral surface, the properties of the adsorbed phase were similar to bulk water. Mulla (1986) reviewed different simulation techniques and suggested that attractive forces become negligible at 10 to 15 Angstroms from the mineral surface. Giese and Costanzo (1986) reviewed the literature on adsorption of water by clay and found a potential range of adsorbed thicknesses between 10 and 100 Angstroms. Henneker (1949, as cited in Economides and Miller, 1985) reports water on glass oriented up to a thickness of 5300 Angstroms. It must also be kept in mind that the electrostatic forces that result in adsorption decrease away from the mineral substrate. Therefore, there is a gradational transition between the adsorbed phase and the bulk fluid rather than an abrupt transition as will be implied in our treatment.

MEASUREMENTS

Because pore space within core from The Geysers is heterogeneous, two different techniques have been identified for its characterization. The first is Scanning Electron Microscopy (SEM). This method has been used to image the mineral-void relationships inside pores. It has the advantage of not disturbing the fine textural features while being capable of high magnification. Measurement of the distribution of pores within a sample has utilized a technique known as Laser Scanning Confocal Microscopy (LSCM). The application of this technique requires that the sample be injected with an epoxy doped with a fluorescent dye. LSCM utilizes a laser to focus at different layers of the sample, allowing three-dimensional imaging of the pores. A convenient aspect of LSCM is that the data are recorded digitally. The remainder of this paper will discuss only the analysis of SEM images of pore interiors, the features we consider most important in determining the volume of water that could be adsorbed.

IMAGE ANALYSIS

Studies that have used SEM imagery in the characterization of rock pore space (Krohn, 1988; Krohn and Thompson, 1986), have relied on brightness maxima, often located at the pore edge, to determine feature boundaries (Fig. 3c and d). Although brightness maxima are often present in SEM images, there are circumstances that sometimes prevent their manifestation. Therefore, this study involved development of other methods to handle SEM data.

Digital image processing of SEM data was approached as a micro-scale remote sensing and geographic information system (GIS) problem. This consisted of the use of digital SEM images, at an 8-bit quantization level, to incorporate 256 gray-scale levels to be used in the classification of pore space by albedo. Classifications were made by digitally overlaying GIS files, consisting of maps of the gray-scale images quantified by albedo, onto the original gray-scale images. The ability to digitally overlay mapped data correlation is the heart of GIS. Two methodologies were utilized in this regard (Fig. 4).

Before the geometry of the pore space could be determined, several preprocessing steps were necessary. Initially, SEM images were scanned into a raster format at a resolution of 300 pixels per inch. The resultant raster gray-scale images were then digitally trimmed to remove the remnants of white photographic paper boundaries and mixed pixels along the edge of the image. The trimmed SEM images were then converted into the tag image file format (TIFF), and imported into ERDAS digital image processing software, where they were converted to an ERDAS gray-scale image file format for further processing and classification.

The first classification method involved the reduction of brightness-value data volume. The original gray-scale images consisted of 8-bit data with an albedo (brightness-value) range from 0 to 255. It was believed that the reduction of this range could simplify the classification process and possibly aid in the development of an automated classification procedure.

To accomplish the data reduction, a single SEM digital image was subjected to an iterative self-organizing data analysis technique (ISODATA), a semi-supervised statistical training algorithm. The ISODATA algorithm is similar to a nearest-neighbor classifier, but generally considered to be superior (Campbell, 1987). This technique generates pixel cluster means according to the following criteria: (1) the maximum number of clusters to be considered, (2) the convergence threshold, (3) the maximum number of iterations to be performed, and (4) the minimum number of pixels allowed in a cluster (ERDAS, Inc., 1991). The cluster means are derived from brightness values, with the cluster generation being a function of pixel homogeneity. This process generated the statistics used on subsequent SEM images.

The cluster means generated in training were then utilized in a final classification scheme. This classification strategy consisted of a parallelepiped (Jensen, 1986; Campbell, 1987) preclassification set to a threshold of ± two standard deviations. Cluster means that were found outside of the ± two standard deviation threshold were assigned to an unclassified category. As the outlier data were less homogeneous than the data classified within the parameters set in the parallelepiped method, and due to the fact that some data may fit into overlapping parallelepiped boundaries, a more robust statistical

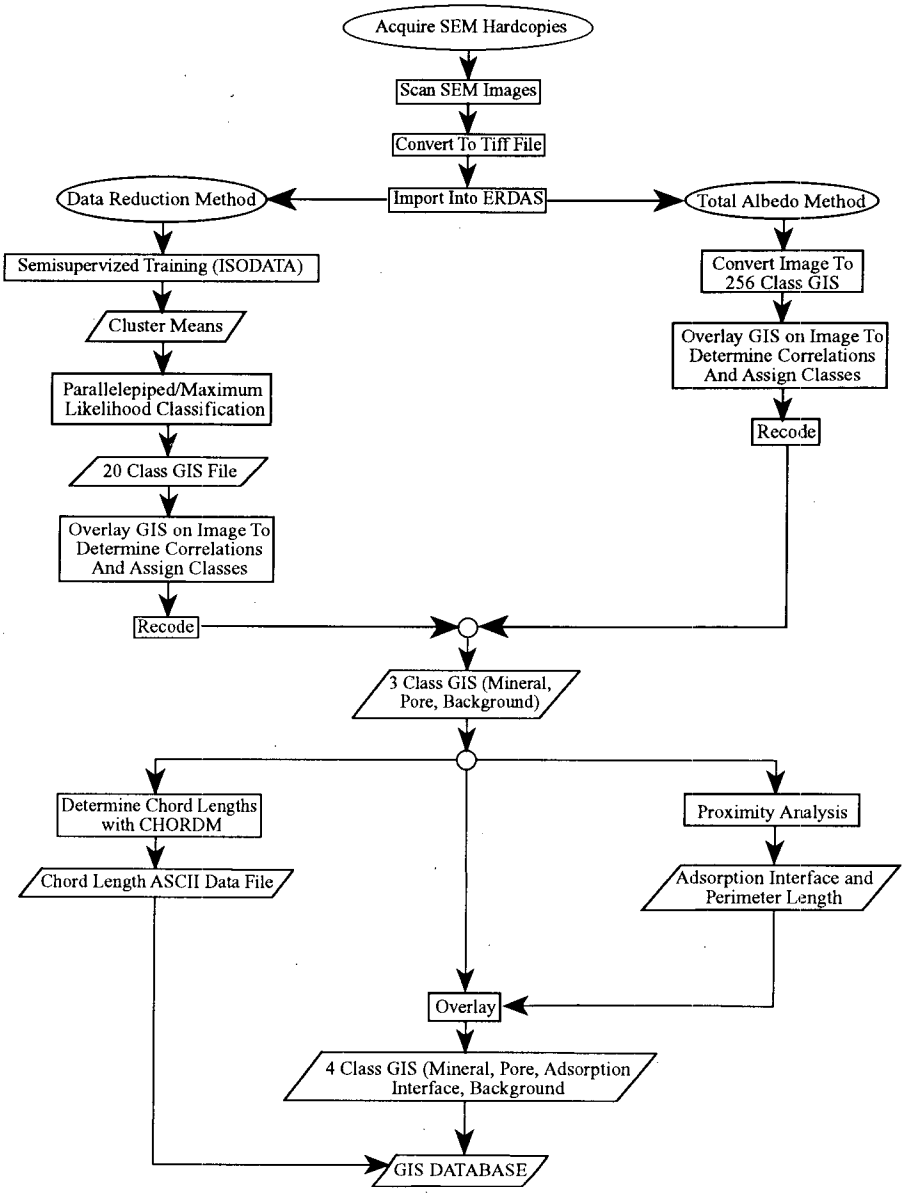

Figure 4. Flow chart for computer assisted porosity determination.

method was utilized to classify the remaining values. The maximum likelihood method was used in this respect (Jensen, 1986; Campbell, 1987). The final output, a twenty class GIS file, consisted of data that had been compressed from 265 to 20 gray-scale levels. Therefore, the albedo data volume was reduced by a factor of 12.19. The twenty-class output GIS file was then utilized to determine which of the new albedo classes best represented solid mineral, pore space, and the interface between the two. The interface is the surface area available for fluid or vapor adsorption. The ISODATA algorithm allows efficient classification as it generates sequential cluster means by albedo level, resulting in gray-scale classes ordered according to brightness values, with class 1 being the closest to black, and class 20 being the closest to white. This 20 gray-scale class GIS file was digitally overlain on the original SEM gray-scale image to determine which classes corresponded with which features. A histogram equalization of the gray-scale image aided in this procedure. Classes 1 - 6 (cluster means of 5.95 - 22.39) were determined to represent pore space best, and classes 7 - 20 (cluster means of 33.44 - 127.67) to represent solid mineral best. The data were then recoded to the two classes indicated above.

This method allows the total automation of all of the above processes. A problem arises in the fact that not all SEM data are consistent. This can be due to scale changes and heterogeneous mineralogy resulting in contrast inconsistencies on the SEM images. Therefore, while data reduction worked very well on a limited number of SEM images, the results were inconsistent on others.

In an attempt to eliminate the problems encountered in the data reduction method, a second, total albedo, approach

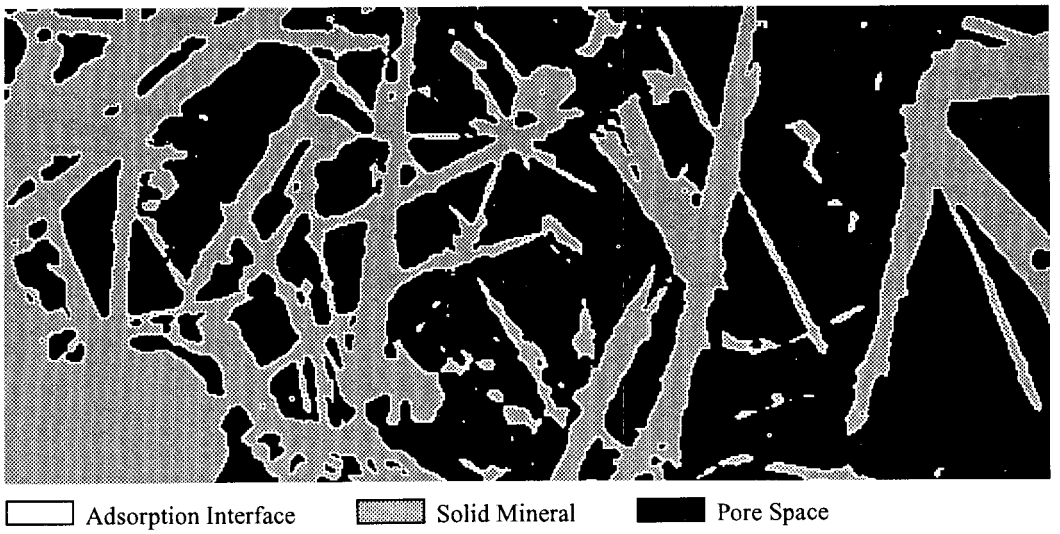

Figure 5. Processed image 02004 (Fig. 3A) with adsorption thickness of 7575 Angstroms

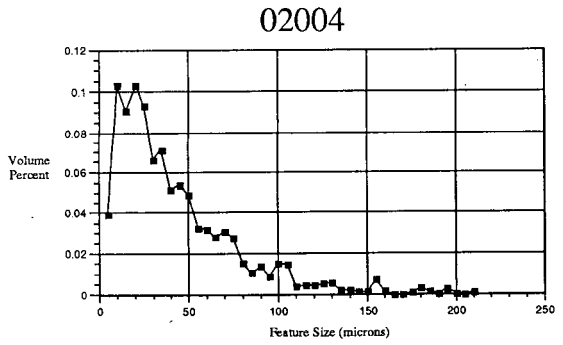

Figure 6. Pore volume relationships from sample 02004 (Fig. 3A)

was developed. In this method, no data reduction was attempted. Therefore, more changes in albedo could be detected. The first step in this method is, again, to transfer scanned SEM images into the ERDAS system.

The gray-scale image is then converted to a GIS file and assigned 256 classes, with class 0 being black, and class 255 being white. The GIS file can then be digitally overlain on the SEM gray-scale image with no further processing. Each of the 256 classes, except zero, are then checked to determine which feature they correspond to. Although there are many more classes to categorize using this method, it was found that it was much more efficient than the data reduction method, as no clustering statistics had to be generated. It was also determined that for the images that did not work well with the data reduction method, each had to be classified as a separate unit. This factor eliminates the possibility of total automation with this method.

The 256-class GIS was then recoded to two classes consisting of solid mineral and pore space. The total albedo method then proceeds in the same manner as the data reduction method. The following methods were applied to both.

The two-class recoded GIS files were used as input to the CHORDM program written by UURI computer specialist Brad Beck. This program measured pore chord lengths which were scaled to microns, and output in ASCII format. The chord lengths were used to determine the statistical distribution of pore dimensions.

The pore space/solid mineral GIS file was then utilized to determine total area of pore space, to determine pore perimeters, and to determine the total length, in microns, scanned by the CHORDM program. Before the statistics of these properties could be compiled, a new class, consisting of adsorption surfaces, had to be generated. It was determined that adsorption surfaces could be estimated by counting the solid mineral pixels at the pore-mineral interface.

To accomplish this task, proximity analysis was utilized. In this process, the area at one pixel depth, immediately adjoining the pore spaces, was determined and reclassified as adsorption interface. Proximity analysis was also utilized to determine the total perimeter of the pore spaces. The ERDAS BSTATS program was then utilized to generate the statistics, which consisted of pore-space area, pore-space perimeter, solid-mineral area, the total adsorption area of the interface between the pore spaces and solid mineral, and the total length of the pixels in the image. Figure 5 is a processed image of sample 02004 (Fig. 3a). The processed image shows solid mineral as stippled, pore space as black, and an adsorbed water layer as white. At this scale, the adsorbed phase is one pixel thick which is equivalent to 7575 Angstroms.

POROSITY DISTRIBUTION

Void space within calcite-dissolution vugs is logarithmically distributed with the greatest volume represented by the lower chord lengths. Figure 6 shows the volume percent as a function of chord length for sample 02004 (Fig. 3A).

Initial observations suggested that the void space in the vugs could be represented by a fractal distribution. The

lengths of chords transecting pore spaces were analyzed using the approach of Krohn (1988). A histogram of chord lengths was constructed using bin sizes appropriate to the scale of the image. These chord lengths were normalized by dividing by the porosity scan length of each individual image. Log-log plots of pore lengths as a function of bin size were prepared. This analysis showed that, for features above 1 micron in size, the distribution of pore volume is not fractal. Sufficient data to analyze feature sizes smaller than this have not been collected at this time.

The objective of this exercise is to estimate the potential liquid reserves due to adsorption. Image analysis provides a measurement of the lengths of chords that traverse pore space and the length of the boundary between the solid and pore. Relative volume calculations of the percent adsorbed fluid assume that the images represented slices of rock that are the thickness of the adsorbed layer. It is also assumed that the total pore space is filled with water resulting in a simple two phase water-adsorbed water relationship. The calculated relative volume of adsorbed water is a function of the magnification of the image. The calculated volume percents were plotted against magnification and then extrapolated to 0. It was found that the actinolite-filled pores had a slightly higher adsorption capacity than epidote-filled pores. The actinolite assemblages supported a 0.005% volume adsorption at an assumed adsorption thickness of 10 Angstroms, 0.05% at 100 Angstroms, and 2.5% at 5300 Angstroms.

CONCLUSIONS

This paper is designed to demonstrate a methodology for using image analysis to determine the proportion of reserves that can be attributed to adsorption in The Geysers reservoir. It should be stressed that this paper is not a comprehensive treatment of matrix porosity since only a few samples have been analyzed in detail. The conclusions from the present work are as follows.

1. Image analysis provides a means for independently measuring porosity distribution and the surface area available for fluid adsorption.

2. Estimates of reserves, using the approach presented here, are highly dependent on the assumed thickness of the adsorbed layer. These data have apparently not been collected for the mineral phases of importance in The Geysers reservoir.

3. The proportion of total water adsorbed to mineral surfaces is small and would not seem to be important in the calculation of total reserves unless extraordinary adsorption thicknesses are present.

ACKNOWLEDGEMENTS

This work was sponsored by the U. S. Department of Energy under contract No. DE/AC07/90ID12929. This support does not constitute a DOE endorsement of the views expressed in this paper. The authors express their appreciation to Wes Martin of Terra Tek for his expert assistance on the Scanning Electron Microscope. We appreciate the technical reviews by P. M. Wright and J. N. Moore of UURI.

REFERENCES

Campbell, J. B., 1987. Image Classification, Introduction to Remote Sensing, Guilford Press: New York, pp. 294-333.

Economides, M. J. and Miller, F. G., 1985, The effects of adsorption phenomena in the evaluation of vapor-dominated geothermal reservoirs: Geothermics, v. 14, p. 3-27.

ERDAS, inc., 1991, Classification, ERDAS Field Guide, pp 105-142.

Giese, R. F. and Costanzo, P. M., 1986, Behavior of water on the surface of kaolin minerals, in Davis, J. A. and Hayes, K. F. (eds.), Geochemical processes at mineral surfaces: American Chemical Society Symposium Series 323, Washington, D.C., p. 37-53.

Gunderson, R. P., 1990, Reservoir matrix porosity at The Geysers from core measurements: Geothermal Resources Council Transactions, v. 14, p. 1661-1665.

He, H. X., Cushman, J. H. and Diestler, D. J., 1987, Molecular dynamics of water near an uncharged silicate surface, in Evans, D. D. and Nicholson, T. J. (eds.), Flow and transport through unsaturated fractured rock: American Geophysical Union Monograph 42, Washington.

Henneker, J. C., 1949, The depth of the surface zone of a liquid: Review Modern Physics, v. 21, p. 322-341.

Hulen, J. B., Nielson, D. L. and Martin, W., 1992, Early calcite dissolution as a major control on porosity development in The Geysers steam field, California--additional evidence in core from Unocal well NEGU-17: Geothermal Resources Council Transactions, v. 16, p. 167-174.

Hulen, J. B., Walters, M. A., and Nielson, D. L., 1991, Comparison of reservoir and caprock core from the northwest Geysers steam field--implications for development of reservoir porosity: Geothermal Resources Council Transactions, v. 15, p.11-18.

Jaroniec, M. and Madey, R., 1988, Physical adsorption on heterogenous solids: New York, Elsevier, 351 p.

Jensen, J. R., 1986. Thematic Information Extraction, *Introductory Digital Image Processing*, Prentice Hall: Englewood Cliffs, pp. 177-233.

Krohn, C. E., 1988, Sandstone fractal and euclidean pore volume distributions: Journal of Geophysical Research, v. 93, p.3286-3296.

Krohn, C. E. and Thompson, A. H., 1986, Fractal sandstone pores: automated measurements using scanning-electron-microscope images: Physical Review B, v. 33, p.6366-6374.

Mulla, D. J., 1986, Simulating liquid water near mineral surfaces: current methods and limitations, in Davis, J. A. and Hayes, K. F. (eds.) Geochemical processes at mineral surfaces: American Chemical Society Symposium Series 323, Washington, D.C., p. 20-36.

Moore, J. N., 1992, Thermal and chemical evolution of the Geysers geothermal system, California: Reprints, Seventeenth Workshop Geothermal Reservoir Engineering, Stanford University.

Nielson, D. L. and Brown, D., 1990, Thoughts on stress around The Geysers geothermal field: Geothermal Resources Council Transactions, v. 14, p. 1685-1690.

Pruess, K. and Narasimhan, T. N., 1982, On fluid reserves and the production of superheated steam from fractures, vapor-dominated geothermal reservoirs: Journal of Geophysical Research, v. 87, p. 9329-9339.

Pruess, K. and O'Sullivan, M., 1992, Effects of capillarity and vapor adsorption in the depletion of vapor-dominated geothermal reservoirs: Reprints, Seventeenth Workshop Geothermal Reservoir Engineering, Stanford University.

Ramey, H. J., 1990, Adsorption in vapor-dominated systems: U. S. Department of Energy Geothermal Program Review VIII, CONF-9004131, p. 63-67.

Thompson, A H., 1991, Fractals in rock physics, in Wetherill, G. W., Albee, A. L. and Burke, K. C., (eds.), Annual Review of Earth and Planetary Sciences, v. 19, p. 237-262.

Truesdell, A. H. and White, D. E., 1973, Production of superheated steam from vapor-dominated geothermal reservoirs: Geothermics, v. 2, p. 154-173.

Williamson, K. H., 1990 Reservoir simulation of The Geysers geothermal field: Proceedings, Fifteenth Workshop on Geothermal Reservoir Engineering, Stanford University, SGP-TR-130, p. 113-123.

Willis, G. F. and Tosdal, 1992, Formation of gold veins and breccias during dextral strike-slip faulting in the Mesquite Mining district, southeastern California: Economic Geology, v. 87, p.2002-2022.